Heat Transfer and Pressure Drop Characteristics of MWCNT/Heat Transfer Oil Nanofluid Flow inside Corrugated Tubes

M.A. Akhavan-Behabadi, M. Karami, and B. Sajadi

***Abstract*—**In the present research work, an experimental study is carried out to investigate the heat transfer and pressure drop characteristics of MWCNT/heat transfer oil nanofluid flow inside horizontal corrugated tubes under uniform wall temperature condition. The results show that tube corrugating shifts the flow regime to the turbulent condition at a lower Reynolds number than the smooth tubes. The acquired data confirm the increase of both heat transfer and pressure drop rates as a result of utilizing nanofluids instead of base fluid. However, corrugating the tubes only decreases the heat transfer rate at low Reynolds numbers. The highest enhancement in the heat transfer rate occurs at the Reynolds numbers in which the flow inside smooth tubes is in the transition regime; where the corrugations make the flow to jump to the turbulent regime.

***Keywords*—** Nanofluid, MWCNT, Heat transfer oil, corrugated tube.

I. Introduction

CONVECTION enhancement techniques represent an unending topic amongst heat transfer research community, logically justifiable due to their benefits in the industry. Enhancement techniques based on artificial roughness have proved to be one of the most effective ones in the heat exchangers.

Artificial roughness techniques are appropriate for the heat transfer rater increment in the turbulent regime, as they contribute to disturbing the thermal boundary layer, while they have proven rather unsuccessful in improving the heat transfer rate in the fully laminar regime.

The momentum transfer mechanism is unavoidably laminar in some cases; therefore the effectiveness of the turbulent heat transfer is inevitably unavailable. Applying artificial roughness techniques would lead to perturb the viscous sub-layer, thence turbulence spots at Reynolds numbers below 2300 result in earlier turbulence phenomena. The recognition of the best enhancement technique will bring about a significant increase in the heat transfer rate within the transition region, this presenting a high potential in applications with highly viscous fluids, e.g. in the petrochemical and food industries [1], [2].

Targanski and Cieslinski [3] provided experimental data on the evaporation of pure R407c and R407c/oil mixture applying two enhanced tubes (micro-finned tube and corrugated tube). Significantly higher average evaporation heat transfer coefficients for were observed the enhanced tubes, particularly for the micro-fin tube. Over the range of tested mass flux, the enhancement factor for the copper micro-finned tube was reported higher than 1. However, in the case of stainless steel corrugated tubes, this ratio was lower than 1.

Dong et al [4] investigated water and oil flows in four corrugated tubes. The enhanced tubes revealed an increase in the tube-side heat transfer coefficient, ranging from 30% up to 120%. In addition, the suggested some correlations based on their results and formerly developed models.

Rozzi et al [5] studied the effect of corrugation on the heat transfer rate with both Newtonian and non-Newtonian fluids. For generalized Reynolds number, ranging from about 800 to the transitional flow regime limit, the helical corrugation significantly enhanced the overall heat transfer; while in the fully developed turbulent flow regime, a moderate overall heat transfer enhancement could be accomplished.

Vicente et al [6] performed an experimental study on a family of corrugated tubes. Corrugated tubes provided up to 250% enhancement in Nusselt number. General correlations were formulated to characterize the studied corrugated tubes. In a search for optimum concentration, Fotukian and Nasr [7] had a broad study on dilute nanofluids. Mixing these two methods (using nanofluids as working fluid and changing flow configuration) was done before [8]-[11], but applying corrugated tube for a nanofluid was not studied nor reported to the knowledge of the authors.

II. Experimental Setup

A schematic diagram of the experimental facility and a corrugated tube are shown in Figs. 1 and 2, respectively. The flow loop consists of a test section, a steam chamber, a cooler, a reservoir, a gear pump, a flow measuring apparatus, (how

Mohammad Ali Akhavan-Behabadi , Center of Excellence in Design and Optimization of Energy Systems, School of Mechanical Engineering, College of Engineering, University of Tehran, Tehran, Iran (corresponding author's phone: +9821-88003328; fax: +9821-88013029; e-mail: akhavan@ut.ac.ir).

Majid Karimi , Center of Excellence in Design and Optimization of Energy Systems, School of Mechanical Engineering, College of Engineering, University of Tehran, Tehran, Iran.

Behrang Sajadi , Center of Excellence in Design and Optimization of Energy Systems, School of Mechanical Engineering, ollege of Engineering, University of Tehran, Tehran, Iran (e-mail: bsajadi@ut.ac.ir).

many) thermocouples and a flow control system. The test section itself is a four-time corrugated copper tube surrounded by a steam chamber to maintain its wall temperature nearly constant. Fig. 3 illustrates the tubes cross section whose specifications are provided in Table 1. The fluid leaving the test section enters the flow measuring device; then it is partially cooled down and is restored in a reservoir. A gear pump drives the flow into a bypass valve to divide the fluid into two separate flows; one of which passes through the test section and the other one bypassed directly to the reservoir. The setup was designed to measure the heat transfer rate as well as the pressure drop throughout the test section. The applied 0.5 mm thick tubes with a length of 1200 mm, were installed horizontally in the experimental setup according to Fig. 1.

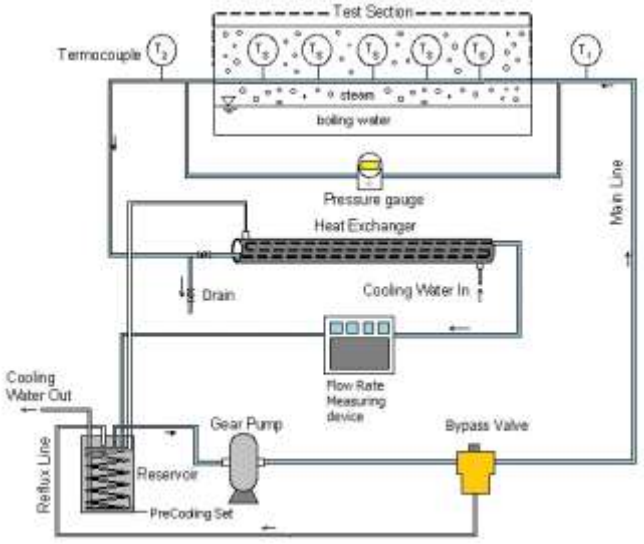

Fig. 1 Schematic view of the experimental setup

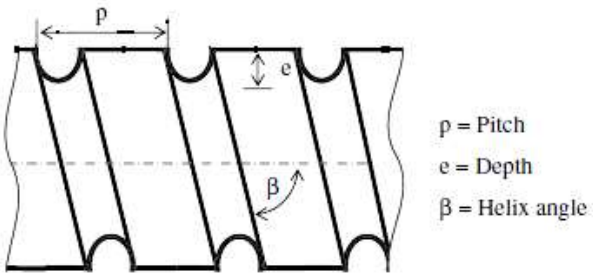

Fig. 2 Geometric parameters of a corrugated tube

TABLE I
SPECIFICATION OF THE TUBES

Tube No.	Diameter prior to corrugation (mm)	Hydraulic diameter (mm)	e (mm)	P (mm)
I	12.7	11.9	1.25	14
II	19	13.2	0.92	14
III	19	15.5	1.1	14

Fig. 3 The cross-section of a four-time corrugated tube

A. Temperature measurement

Two calibrated RTD PT 100 type temperature sensors with ±0.1°C accuracy were designated to measure the inlet and outlet temperatures of the fluid. In addition, five K-type (Chromel – Alumel) thermocouples were mounted on the surface of the test sections at 200, 400, 600, 800, and 1000 mm from the beginning of the test section to measure the wall temperatures and to ensure that the surface temperature is uniform along the test section. The accuracy of K-type thermocouples was ±1.5°C. Each thermocouple was attached individually to a separate Hyundai indicator thermometer. Data were recorded whenever the system achieved the steady state condition, as the temperatures remained constant for at least 20 minutes. Table 2 provides the error of all measuring instruments.

TABLE II
RANGE AND ACCURACY OF THE MEASURING INSTRUMENTS

Description	No.	Model	Range	Accuracy
Inlet temp.	1	RTD PT 100	-200-500 °C	±0.1 °C
Outlet temp.	1	RTD PT 100	-200-500 °C	±0.1 °C
Surface temp.	5	Type K thermocouple	-100-1370 °C	±1.5 °C
Flow rate	1	Piusi K44	5-120 l/s	±0.1 l/s
Pressure drop	1	PMD-75	0.01-40 mbar	±0.075

B. Fluid flow measurement

The flow measuring device was a K44 Piusi rotating disk oil flow meter. There was an adjusting screw to calibrate the flow meter for each type of fluid with the bucket and stopwatch method. The flow rate was measured directly from the time required for a specified amount of oil (typically 10 liters) to pass the flow meter. The bypass valve was used to regulate the flow rate in the main line. When all the experiments associated with a fluid were conducted, the suction line was opened and the flow loop, including the inner wall of the tested corrugated tubes and all other connecting lines, was completely cleaned using compressed air. It was necessary to clean the whole cycle just after finishing each test, as nanoparticles may be settled down and change the nanofluid specifications. In addition, for the sake of best accuracy, it was decided to wash the whole cycle with the pure base fluid whenever the working fluid was changed. This process prevents MWCNTs from depositing on the inner wall of tubes before starting the experiments.

C. Preparation of the base fluid and nanofluids

Heat transfer oil was selected as the base fluid as it may

work in closed thermodynamic cycles under high temperatures, typically 100 °C to 300 °C, and due to its wide industrial applications. In addition, Multi-Walled Carbon NanoTube (MWCNT) was utilized as an additive. Table 3 shows the properties of the applied nanoparticles. 0.05, 0.1 and 0.2% wt. equivalent to 0.031, 0.062 and 0.125% vol. concentrations were prepared by dispersing a specific amount of MWCNT in the heat transfer oil by means of an electrical blender. To break large clusters of nanoparticles in the fluid, a UPS400 ultrasonic processor (400 W, 24 kHz) was used for 6 hours so that a stable suspension was achieved. No surfactant was applied due to their probable influence on the effective thermal conductivity of the nanofluid. Several observations confirmed that the nanoparticles were uniformly dispersed for 24 hours without sedimentation.

TABLE III
PROPERTIES OF THE MWCNT NANOPARTICLES

Parameter	Value
Purity	95%
Effective area (m2 /gr)	270
Length (μm)	1-10
Outer diameter (nm)	5-20
Inner diameter (nm)	2-6
Thermal conductivity (W/mK)	1500
Number of walls	3-15
Apparent density (gr/cm3)	0.15-0.35
Loose agglomerate size (mm)	0.1-3

D. Validation of the experimental setup

The setup was used to measure Nusselt number and friction factor of base fluid flowing in smooth tube. The results fall within ±15% of the empirical prediction values suggested by Kays [1993].

III. UNCERTAINTY ANALYSIS

The uncertainty in calculating the fluid flow parameters has been conducted using the values presented in Table 2, based on the Kline and McClintock's method [12]. As a consequence, the uncertainties of heat transfer coefficient, Reynolds number, and Nusselt number were 8.7, 4.2, and 8.4%, respectively.

IV. DATA PROCESSING

As defining a diameter for corrugated tubes is pointless, their geometry is expressed using the hydraulic diameter concept:

$$D = \frac{4A}{P} \tag{1}$$

Equations (2) to (5) are introduced to evaluate the heat transfer coefficient of the nanofluid flows:

$$\mathrm{Re} = \frac{\bar{V}D}{v} \tag{2}$$

$$\dot{m}c_p\left(T_{out} - T_{in}\right) = \bar{h}A \times LMTD \tag{3}$$

$$LMTD = \frac{\left(T_s - T_{in}\right) - \left(T_s - T_{out}\right)}{\ln\frac{\left(T_s - T_{in}\right)}{\left(T_s - T_{out}\right)}} \tag{4}$$

$$\overline{Nu} = \frac{\bar{h}.D}{k} \tag{5}$$

In all cases, an average temperature between inlet and exit was used as a reference temperature to determine the fluid properties. As the viscosity strongly depends on the temperature, Sieder and Tate correction factor, $(\mu/\mu_w)^{0.14}$, is also applied in this study [13].

V. RESULTS AND DISCUSSION

After performing the experiments on the corrugated tubes and correcting the Nusselt number with the above mentioned approach, the results are compared with the available data for smooth tubes. Figs. 4 and 5 depict the Nusselt number variation with the Reynolds number for the base fluid and the nanofluid flows with various concentrations in the corrugated tubes type I and III, respectively.

It is clear that at a certain range of Reynolds number, the heat transfer rate of the nanofluid flow is more than the base fluid. This happens because based on the observations during the experiments, the bulk temperature of the fluid increases with the Reynolds number. Therefore, at low Reynolds numbers the high viscosity of oil prevents the nanoparticles from free movement. On the contrary, as the Reynolds number increases, the oil viscosity drops significantly and the oil loses its control on the nanoparticle movements. In addition, at the high flow rates, the dispersion effects and the chaotic movement of the particles are intensified which causes the temperature profile to be more flat and leads to an increment in the heat transfer coefficient. So, the more concentration of nanofluid, the higher dependence of the Nusselt number upon the Reynolds number. Though not significant, this nuance is revealed in the power equation, see Eq. (6). As shown in these figures, two main regimes may be detected for the nanofluid flows inside the tested corrugated tubes. For the Reynolds number less than almost 500, the slope of Fig. 4 is considerably less than for Re>500. This provides that around the Reynolds number of 500, the flow becomes turbulent. Comparing Figs. 4 and 5, one can conclude that the flow in tube type III undergoes the transition to turbulence in a higher Reynolds number than tube type I. The reason of such difference is due to the geometric characteristics of the corrugated tubes; the tube type I possesses higher depth-to-diameter and pitch-to-diameter ratios. Overall, it could be argued that increasing nanoparticles mass concentration can enhance the heat transfer rate. In the tube type I, with 0.05% increment the nanoparticles mass concentration, the heat transfer augments 7%. The enhancement is 16 and 31% for the nanoparticle mass concentrations of 0.1 and 0.2% wt., respectively. Having 0.2% wt. nanofluid flows, the highest heat transfer augmentation is 34% inside the tube type II, whereas the corresponding value for the tube type III is almost 40%. In should be also noted that the unexpected change of the

Nusselt number at Re≈300 for the tube type III may be due to transition of the flow regime.

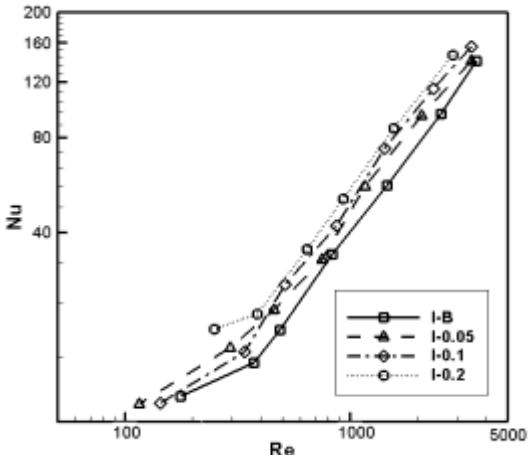

Fig. 4 The Nusselt number in corrugated tube type I

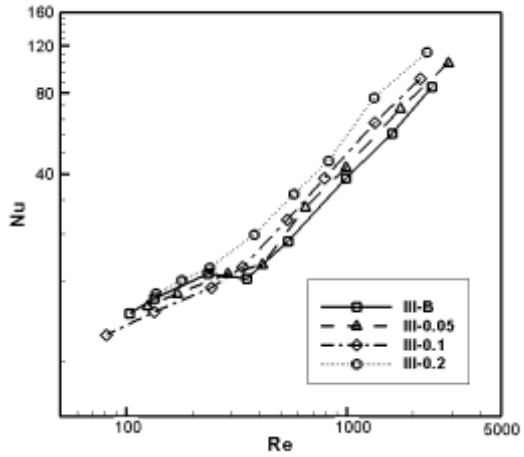

Fig. 5 The Nusselt number in the corrugated tube type III

Fig. 6 shows the variations of the Nusselt number with respect to the Reynold number for the base fluid flow in different tubes. As seen from the figure, the flow is laminar in the smooth tube. For Re<500, the heat transfer in the corrugated tubes is less than the smooth one, since the chaos caused by the tube corrugations delays the development of the mixed convection regime. Such phenomenon is also reported in the vast majority of previous researches on corrugated tubes [3]-[6], [14].Variation of the Nusselt number versus the Reynolds number are shown in Figs. 7 and 8 for nanofluids with the mass concentration of 0.1 and 0.2% wt. in different types of tube. The exact trend which was observed in Fig. 6 for the base fluid flow is repeated in Figs. 7 and 8 in the case of nanofluid flow. Considering Figs. 6-8, it is clear that the fluid flow inside tube type I, having the largest roughness, shows the highest rate of heat transfer. The maximum enhancement in the heat transfer rate for the base fluid flow in corrugated tubes type I, II and III is 137, 115 and 99%, respectively. This increment was determined to be 133, 131 and 127% for the nanofluid flow with the mass concentration of 0.1% wt. The Nusselt number in the base fluid flow is more subject to the corrugation parameters, while the nanofluid with 0.1% mass concentration less depends upon these factors. This can be attributed to the fact that the corrugations and the nanoparticles enhance the heat transfer rate in a similar/parallel manner.

Considering the different values of heat transfer in various experiments, the fluid temperature inevitably differs. Regarding the high dependency of Prandtl Number on temperature in oils, it is customary to present variations of parameter $Nu/Pr^{0.4}$ with respect to Reynolds number to show the independence of the results on the variations of Prandtl number, see Fig. 9.

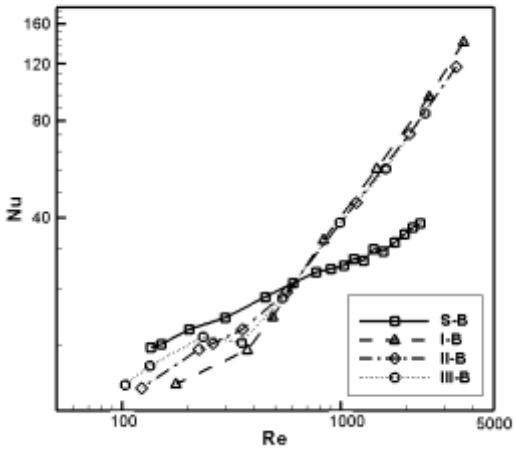

Fig. 6 The Nusselt number of the base fluid flow

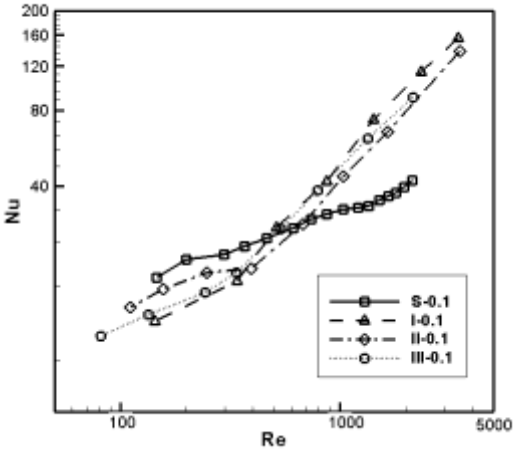

Fig. 7 The Nusselt number for 0.1% wt. nanofluid flow

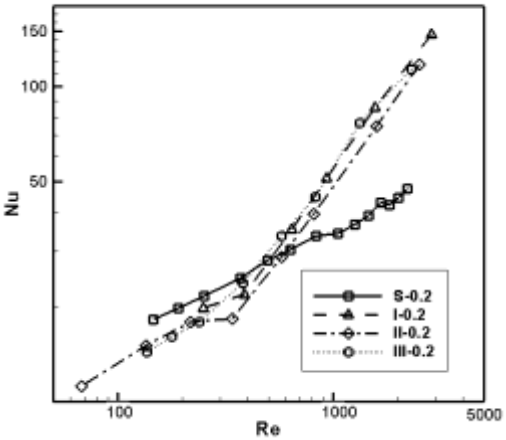

Fig. 8 The Nusselt number for 0.2% wt. nanofluid flow

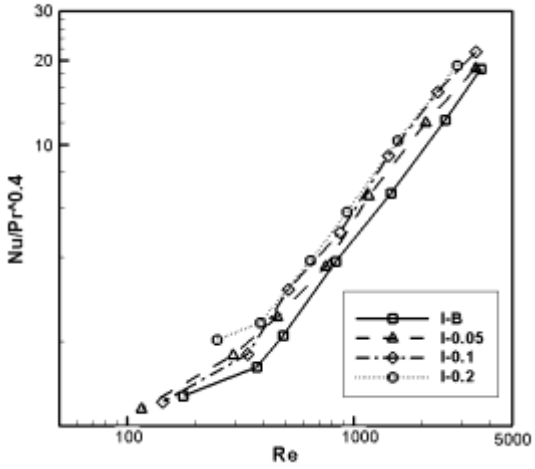

Fig. 9 Independence of the parameter $Nu/Pr^{0.4}$ upon variations of Prandtl number

Based on [2] recommendation, a power equation has been used to correlate the Nusselt number. Based on the experimental data and the least square method, the following correlation has been developed to predict the Nusselt number inside corrugated tubes:

$$Nu = 0.023\,\mathrm{Re}^{m}\,\mathrm{Pr}^{0.4}\left(\frac{\mu}{\mu_w}\right)^{0.14}\left(\frac{d}{L}\right)^{0.33}\left(\frac{e}{D}\right)^{0.33}\left(\frac{P}{D}\right)^{-0.14} \quad (6)$$

where, m depends on the fluid type and can be obtained from Table 4.

TABLE IV
VALUES OF M

Fluid	Base fluid	0.05%	0.1%	0.2%
m	1.083	1.096	1.112	1.127

When the boundary condition is constant temperature, the fluid properties at the wall temperature differ from the bulk ones, significantly. Thus, the Sider and Tate correction factor $(\mu/\mu_w)^{0.14}$ is added to take these deviations into account. The square correlation coefficient of (6) was determined as 0.95. As shown in Fig 10, the data predicted by (6) falls within ±15% of the acquired experimental values.

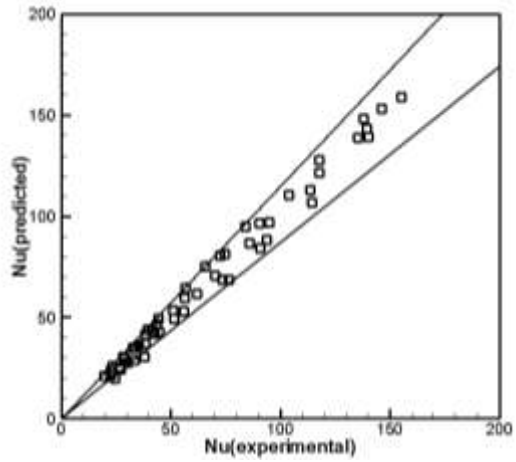

Fig. 10 The predicted Nusselt number vs. the experimental values

Fig. 11 displays the friction factor of the base fluid. After a certain value of Reynolds number, the friction factor becomes independent from the Reynolds number. This fact is readily obvious in the Moody's diagram. The sole difference between smooth tubes and corrugated ones is that in smooth tubes this phenomenon happens in a higher Reynolds number than corrugated one. Turbulence is much further in the corrugated tubes; also the transition to turbulent regime occurs in a lower Reynolds number.

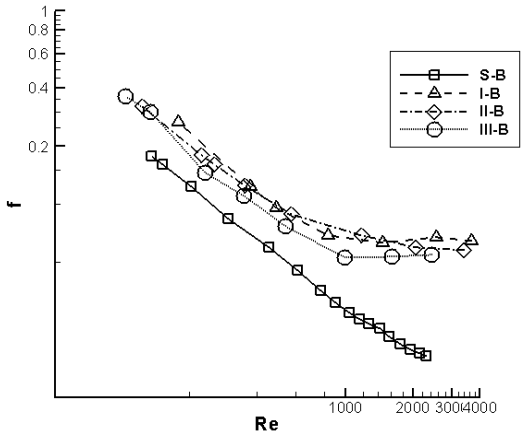

Fig. 11 Darcy friction factor for the base fluid

The mentioned order is observable in nanofluids. Fig. 12 illustrates the Darcy friction factor (f) for the nanofluid of 0.1% mass concentration.

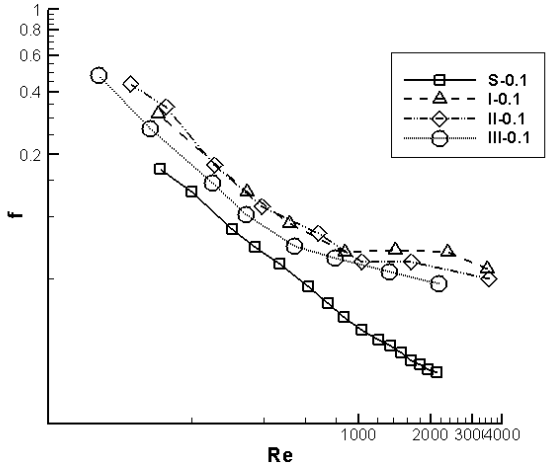

Fig. 12 Darcy friction factor for the 0.1% wt. nanofluid

A power law equation has been designated for the Darcy friction factor. As the flow is hydrodynamically fully developed, no correction is needed. Regarding the method proposed by [13], all the necessary properties for calculations were determined in surface temperature.

$$f = 1.481\,\mathrm{Re}^{-0.228}\left(\frac{e}{D}\right)^{0.172}\left(\frac{P}{D}\right)^{-0.275} \quad (7)$$

The square correlation coefficient of (7) was determined 0.9, and the data predicted by (7) falls within ±16% of the acquired experimental values, see Fig. (13).

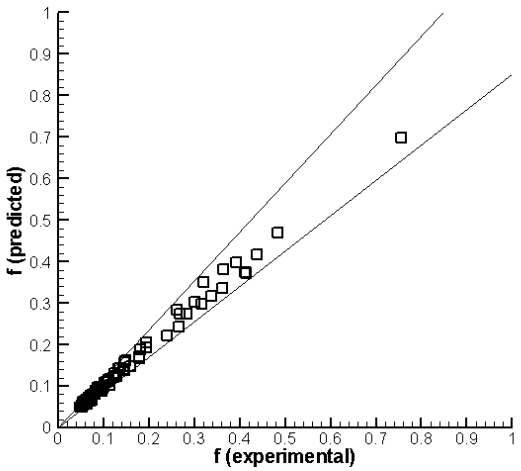

Fig. 13 Predicted friction factor versus the experimental values

VI. Conclusion

In this research, the effect of using corrugated tubes on the heat transfer and pressure drop of MWCNT/heat transfer oil nanofluid was studied experimentally. The results were as follows:

- At a certain range of Reynolds number, the heat transfer rate of the nanofluid flow is more than the base one; shows a rising trend with the nanoparticles mass concentration.
- The best range of Reynolds number for using corrugated tubes is over 500. In the lower Reynolds numbers, corrugation of the tubes acts reversely and reduces the heat transfer rate.
- Corrugating the tubes could increase the Nusselt number up to 137%. The maximum increment in the heat transfer rate was observed for tube type I, which had the largest ratio of depth to diameter.
- The Nusselt number of the base fluid flow is more sensitive to the corrugation parameters; however, the nanofluid with 0.1% mass concentration less depends upon these factors.
- Corrugation may work almost similar to increasing the roughness in smooth tubes. This fact was observable in figures depicting the trend of Darcy's friction factor. The more chaotic the parameters of corrugation could make the flow, the greater the increase of Darcy factor will be, a phenomenon which was detected in the nanofluid of any concentration.

Acknowledgment

The authors would like to express their thanks to the Center of Excellence in Design and Optimization of Energy Systems, College of Engineering, University of Tehran for the financial supports through the set-up construction and research implementation and also the center of excellence in design and optimization of energy systems.

References

[1] S. Kakaç, and S. Pramuanjaroenkij, "Review of convective heat transfer enhancement with nanofluids," *International Journal of Heat and Mass Transfer*, vol. 52, pp. 3187-3196, 2009.

[2] S. Rainieri, F. Bozzoli, and G. Pagliarini, "Experimental investigation on the convective heat transfer in straight and coiled corrugated tubes for highly viscous fluids: Preliminary results," *International Journal of Heat and Mass Transfer*, vol. 55, pp. 498-504, 2012.

[3] W. Targanski, and J.T. Cieslinski, "Evaporation of R407C/oil mixtures inside corrugated and micro-fin tubes," *Applied Thermal Engineering*, vol. 27, pp. 2226-2232, 2007.

[4] Y. Dong, L. Huixiong and C. Tingkuan, "Pressure drop, heat transfer and performance of single phase turbulent flow in spirally corrugated tubes," *Experimental Thermal and Fluid Science*, vol. 24, pp. 131-138, 2001.

[5] S. Rozzi, et al., "Heat treatment of fluid foods in a shell and tube heat exchanger: Comparison between smooth and helically corrugated wall tubes," *Journal of Food Engineering*, vol. 79, pp. 249-254, 2007.

[6] P.G. Vicente, A. Garcia and A. Viedma, "Experimental investigation on heat transfer and frictional characteristics of spirally corrugated tubes in turbulent flow at different Prandtl numbers," *International Journal of Heat and Mass Transfer*, vol. 47, pp. 671-681, 2004.

[7] S.M. Fotukian and M. Nasr Esfahany, "Experimental study of turbulent convective heat transfer and pressure drop of dilute CuO/water nanofluid inside a circular tube," *International Communications in Heat and Mass Transfer*, vol. 37 (2), pp. 214-219, 2010.

[8] S.M. Hashemi and M.A. Akhavan-Behabadi, "An empirical study on heat transfer and pressure drop characteristics of CuO-base oil nanofluid flow in a horizontal helically coiled tube under constant heat flux," *International Communications in Heat and Mass Transfer*, vol. 39, pp. 144-151, 2012.

[9] M.A. Akhavan-Behabadi and P. Razi, "Experimental Investigation on Heat Transfer and Pressure Drop of CuO-Base Oil Nanofluid Flow in Flattened Tubes under Constant Heat Flux," in *International Conference on Nanotechnology: Fundamentals and Applications*, 2012, Paper No. 372.

[10] M.A. Akhavan-Behabadi, M. Fakoor Pakdaman and M. Ghazvini, "Experimental investigation on the convective heat transfer of nanofluid flow inside vertical helically coiled tubes under uniform wall temperature condition," *International Communications in Heat and Mass Transfer*, vol. 39, pp. 556-564, 2012.

[11] D. Ashtiani, M.A. Akhavan-Behabadi and M. Fakoor Pakdaman, "An experimental investigation on heat transfer characteristics of multi-walled CNT-heat transfer oil nanofluid flow inside flattened tubes under uniform wall temperature condition," *International Communications in Heat and Mass Transfer*, vol. 39, pp. 1404-1409, 2012.

[12] S.J. Kline and F.A. Mcclintock, "Describing uncertainties in single-sample experiments," *Mechanical Engineering*, vol. 75, pp. 3-8, 1953.

[13] W.M. Kays, *Convective Heat and Mass Transfer*, McGraw-Hill, pp. 233-292, 1993.

[14] A. García, J.P. Solano, P.G. Vicente and A. Viedma, "The influence of artificial roughness shape on heat transfer enhancement: Corrugated tubes, dimpled tubes and wire coils," *Applied Thermal Engineering*, vol. 35, pp. 196-201, 2012.